Acta Crystallographica Section D
Biological Crystallography
ISSN 0907-4449

The impact of Glu→Ala and Glu→Asp mutations on the crystallization properties of RhoGDI: the structure of RhoGDI at 1.3 Å resolution

Agnieszka Mateja,[a] Yancho Devedjiev,[a] Daniel Krowarsch,[b] Kenton Longenecker,[a] Zbigniew Dauter,[c] Jacek Otlewski[b] and Zygmunt S. Derewenda[a]*

[a]Department of Molecular Physiology and Biological Physics, University of Virginia, Charlottesville, Virginia 22908, USA, [b]Institute of Biochemistry and Molecular Biology, University of Wroclaw, 50-137 Wroclaw, Poland, and [c]Synchrotron Radiation Research Section, Macromolecular Crystallography Laboratory, NCI, Brookhaven National Laboratory, Upton, NY 11973, USA

Correspondence e-mail: zsd4n@virginia.edu

Received 9 May 2002
Accepted 5 August 2002

PDB Reference: RhoGDI, 1kmt, r1kmtsf.

It is hypothesized that surface residues with high conformational entropy, specifically lysines and glutamates, impede protein crystallization. In a previous study using a model system of Rho-specific guanine nucleotide dissociation inhibitor (RhoGDI), it was shown that mutating Lys residues to Ala results in enhanced crystallizability, particularly when clusters of lysines are targeted. It was also shown that one of these mutants formed crystals that yielded diffraction to 2.0 Å, a significant improvement on the wild-type protein crystals. In the current paper, an analysis of the impact of surface mutations replacing Glu residues with Ala or Asp on the stability and crystallization properties of RhoGDI is presented. The Glu→Ala (Asp) mutants are generally more likely to produce crystals of the protein than the wild-type and in one case the resulting crystals yielded a diffraction pattern to 1.2 Å resolution. This occurs in spite of the fact that mutating surface Glu residues almost invariably affects the protein's stability, as illustrated by the reduced ΔG between folded and unfolded forms measured by isothermal equilibrium denaturation. The present study strongly supports the notion that rational surface mutagenesis can be an effective tool in overcoming problems stemming from the protein's recalcitrance to crystallization and may also yield dramatic improvements in crystal quality.

1. Introduction

Crystallization often remains a limiting step in X-ray diffraction analysis of proteins and may be a serious impediment to high-throughput characterization of the proteome. The typical approach to protein crystallization is to screen a broad spectrum of conditions and often to additionally optimize conditions once microcrystals are identified. Precipitant, pH, protein concentration, ionic strength *etc.* all serve as variables in the process, but in most cases the protein sample is constant. Another strategy is to assay a selection of homologous proteins from a number of species, an approach pioneered by J. C. Kendrew (Kendrew *et al.*, 1954), when he selected sperm whale myoglobin as the subject of his study. Modification of the protein, typically truncation by limited proteolysis or recombinant methods, is also a common practice, particularly when isolated domains of large multidomain proteins are a target. Chemical modifications are rarely used with success, but at least two impressive examples are known: myosin subfragment 1, crystallized following reductive methylation of lysines (Rayment *et al.*, 1993) and G-actin in complex with ADP, covalently modified with the fluorescent probe tetramethylrhodamine-5-maleimide (TMR) on Cys374 (Otterbein *et al.*, 2001). Finally, it is possible to modify the surface properties of any protein by site-directed mutagenesis. The

© 2002 International Union of Crystallography
Printed in Denmark – all rights reserved

dramatic impact of even single-site mutants on the crystallizability of a protein was initially demonstrated with thymidylate synthase (McElroy *et al.*, 1992). However, surface mutagenesis has never become a routine method, largely because rational application of this strategy is not straightforward.

We hypothesized that mutagenesis to alanine of those surface residues that have high conformational entropy may promote crystallization by generating epitopes which could be incorporated in crystal contacts without entropic penalty. Two types of amino acids constitute suitable targets: Lys and Glu. Both amino acids have high conformational entropy and both are almost exclusively located on the surface of proteins. Thus, even without the knowledge of the tertiary fold of a given protein, it is possible to target its surface by selecting Lys and/or Glu-rich peptides. Admittedly, Lys→Ala and Glu→Ala mutations not only reduce the excess surface entropy; they also remove charges and alter the protein's isoelectric point and solubility properties, all of which may contribute to the change in the protein's behavior in crystallization assays.

We chose the globular domain of human Rho-specific guanine dissociation inhibitor (RhoGDI) as the model system. This is a cytosolic protein with high Lys and Glu content (~20% of the total amino acids) which is difficult to crystallize. Its structure was originally solved at 2.5 Å resolution with crystals exhibiting high symmetry with three molecules in the asymmetric unit (Keep *et al.*, 1997). Using the Lys→Ala strategy and single as well as multiple mutants, we were able to generate several novel crystal forms, one of which diffracted to 2.0 Å resolution (Longenecker, Garrard *et al.*, 2001). Furthermore, we showed that crystal contacts often incorporate the epitopes which carry the mutated sites, thus lending credibility to the notion of a causal link between the types of mutations and successful crystallization. More recently, we crystallized a novel protein, the RGSL domain of PDZRhoGEF, using a mutant containing three changes: K463A, E465A and E466A (Longenecker, Lewis *et al.*, 2001; Garrard *et al.*, 2001). As was the case with the Lys→Ala mutants of RhoGDI, the mutated epitope was found to be directly involved in some of the key crystal contacts.

In the present study, we return to the RhoGDI model system and analyze the impact of Glu→Ala and Glu→Asp mutations, single and multiple, on the protein's stability and ability to form crystals (Fig. 1). We show that the use of surface mutations of this type also enhances the chances of obtaining X-ray quality crystals and report the structure of a double mutant E(154,155)A of RhoGDI for which high-resolution data (1.25 Å) were obtained. We conclude that rational surface mutagenesis can lead not only to crystals of proteins otherwise recalcitrant to crystallization, but also to marked improvement in the quality of the crystals.

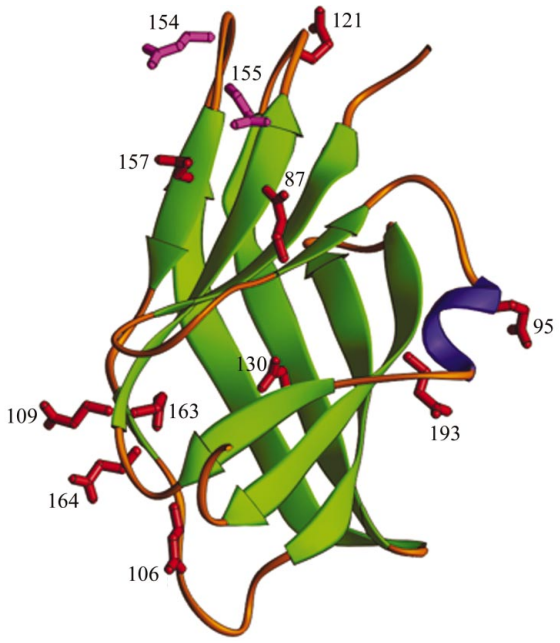

Figure 1
A view of the RhoGDIΔ66 fragment with glutamates shown in full and colored gold. The two sites which were mutated in the highly diffracting crystal form are shown in pink. The sites are numbered according to the amino-acid sequence of the full-length protein. The figure was prepared using *RIBBONS* (Carson, 1991).

2. Methods

2.1. Production and crystallization of RhoGDI mutants

Site-directed mutagenesis was performed using the QuikChange mutagenesis system (Stratagene). The N-terminally truncated form of the RhoGDI, RhoGDIΔ66N, was used as a template. Single mutagenic primers were designed to introduce single, double and triple mutations of the Glu→Ala and Glu→Asp type. Only those double mutants where mutated residues are distant in the sequence were prepared by two-stage mutagenesis of single-mutation-carrying plasmids. All primers were purchased from Life Technologies and used after dissolving in distilled water. DNA manipulations and protein expression were performed in *Escherichia coli* strain XL2Blue (Stratagene).

Mutants of RhoGDIΔ66N were expressed as fusion proteins with 26 kDa glutathione *S*-transferase (GST) and purified from lysed cells under non-denaturing conditions by GST affinity chromatography. The expression vector was a Pharmacia pGEX4T1 derivative with an rTEV cleavage site (Sheffield *et al.*, 1999). Expression of fusion proteins was carried out in 2–4 l of cultures in LB medium containing 2% ethanol and incubated at 310 K until the cells reached log phase (OD_{600} of 0.4–0.6), when expression was induced by the addition of IPTG (final concentration 500 μ*M*). Cultures were grown for a further 16 h at 296 K and cells were harvested by centrifugation at 6000 rev min^{-1}. Cells were resuspended in 50 m*M* Tris pH 8.5 with 300 m*M* NaCl and lysed by sonication. Cell debris and insoluble proteins were separated by centrifugation at 16 000 rev min^{-1} for 60 min and clear supernatant was applied to 10 ml glutathione-Sepharose columns (Pharmacia) pre-equilibrated with 100 ml of GST buffer. Proteins were allowed to bind to the column for 1 h at 277 K. Columns

Table 1
Results of the crystallization of Glu→Ala and Glu→Asp mutants of RhoGDIΔ66.

CSI, Crystal Screen; CSII, Crystal Screen II; the numbers correspond to the numbers of solutions as found in Hampton Research instructions. In each line, bold or italic font correlate conditions and diffraction limit for a tested crystal.

Δ66 RhoGDI	CSI	CSII	Tested for diffraction	d_{min} (Å)
E87A	17	26	Yes	
E155A	—	26	—	
E163A	—	26	—	
E154,155A	**4**, *17*	14	Yes	**2.8**, *1.2*
E163,164A	—	26	—	
E154,155,157A	**4**, 15, 32, 38, 39	14, 22, 25, 30, 38	Yes	**2.8**
E95A	—	14	—	
E109A	15	**26**	Yes	**3.0**
E193A	—	26	—	
E87, 163A	—	26	—	
E87, 155A	4, 15	—	—	
E87D	15	26	—	
E155D	—	14	—	
E163D	—	—	—	
E163,164D	15	26	—	
E154,155D	—	14	—	

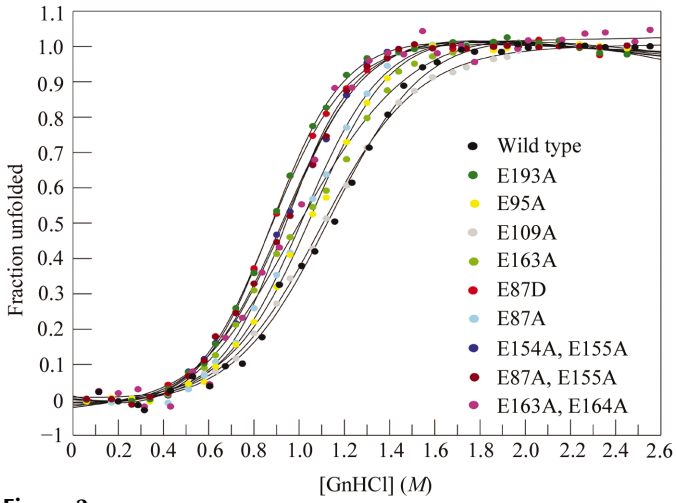

Figure 2
Normalized chemical denaturation curves of GDI wild type and its mutants at pH 8.5 and 294 K. The transitions were monitored by the increase of fluorescence at 334 nm on excitation at 276 nm.

were washed with 2 l of GST buffer. Fusion proteins were recovered from the matrix under mild elution conditions (GST buffer containing 10 m*M* glutathione). The presence of the GST fusion protein was analyzed by SDS–PAGE on 12% polyacrylamide gels in a Laemmli buffer system. The GST tag was removed by incubation with rTEV protease (100 units per 50 mg of protein; Life Technologies) at 283 K. The contaminating GST tag was removed by passing the rTEV-treated protein mixture through another glutathione-Sepharose column. The rTEV protease and residual GST were removed by size-exclusion chromatography (Superdex 75 column).

Proteins were crystallized by the vapor-diffusion method using Crystal Screen I and Crystal Screen II kits from Hampton Research. The sitting drop consisted of 1 µl of protein solution at a concentration of 15–20 mg ml^{-1} and 1 µl of screen solution. The vapor-diffusion trials were carried out using CompactClover 96 well plates (Emerald Biostructures), which were sealed by clear plastic tape. CompactClover plates were chosen to minimize the required volume of the screen solution. Screens were stored in a temperature-controlled environment at 294 K. Optimization was carried out by the hanging-drop vapor-diffusion method at 294 K using VDX 24-well plates. Each well was filled with 500–750 µl of the crystallization solution. In this case, crystals usually appeared within one week.

2.2. Stability measurements of RhoGDI and selected Glu→Ala mutants

The stability of RhoGDI and of its mutants was assessed by isothermal equilibrium denaturation in GnHCl, performed on a FP-750 spectrofluorimeter (Jasco) at 294 K. Protein samples (0.1 µ*M*) in 25 m*M* Tris pH 8.5 were equilibrated for 24 h at 294 K with various concentrations of GnHCl. Excitation at 276 nm and emission at 334 nm were used to maximize the denaturation signal. The apparent free-energy change in the absence of GnHCl ($\Delta G_{\rm den}^{\rm H_2O}$) was determined by fitting the fluorescence intensity change (F) at a particular concentration of GnHCl to the equation (Santoro & Bolen, 1992)

$$F = \frac{a_n + b_n[\mathrm{GnCl}] + a_u + b_u[\mathrm{GnCl}]\exp\{(m[\mathrm{GnCl}] - \Delta G_{\rm den}^{\rm H_2O})/RT\}}{\exp\{(m[\mathrm{GnCl}] - \Delta G_{\rm den}^{\rm H_2O})/RT\}},$$

where $a_n + b_n$[GnHCl] and $a_u + b_u$[GnHCl] describe fluorescence intensity changes of the native and denatured state, respectively, and m is a measure of a linear dependence of $\Delta G_{\rm den}$ on [GnHCl]. Analysis of the data was performed using the *PeakFit* software (Jandel Scientific Software).

2.3. Crystallographic analysis of the E154A, E155A mutant

2.3.1. Δ66 E(154,155)A crystal structure determination. Crystals were harvested in a stabilizing cryosolution (26% PEG 4000, 100 m*M* Tris pH 8.5, 200 m*M* $LiSO_4$ and 20% glycerol) and quickly frozen by plunging them into liquid nitrogen. X-ray diffraction data were collected from a single frozen crystal at the Brookhaven National Laboratory NSLS beamline X9B using an ADSC Quad CCD detector. High-resolution data were collected and merged with data collected on a second pass at shorter exposure times. Reflections were integrated and scaled using *HKL*2000 (Otwinowski & Minor, 1997) and intensities were converted to structure-factor magnitudes using *TRUNCATE* (French & Wilson, 1978). The structure was solved by molecular replacement using *AMoRe* (Navaza, 1994) and a previously determined structure of RhoGDIΔ66 (PDB code 1fso) as a search model. Two orientations yielded values (correlation coefficients of 22.3 and 21.6 for data in the resolution range 15–3.5 Å) significantly higher than other solutions for the rotation function. The relative positions of the two molecules were readily found in the translation search; rigid-body fitting to data in the resolution range 15–3.3 Å yielded a correlation coefficient of

Table 2
Table of elementary X-ray data for crystals.

Values in parentheses are for the highest resolution shell.

	E(109)A	E(154,155)A	E(154,155,157)A	WT-Δ66
Space group	*C*2	*R*32	*R*32	*R*32
Unit-cell parameters				
a (Å)	162.9	129.6	130.4	129.2
b (Å)	62.8	129.6	130.4	129.2
c (Å)	64.9	166.6	163.7	164.2
α (°)	90	90	90	90
β (°)	93.9	90	90	90
γ (°)	90	120	120	120
Resolution	3.0 (3.1–3.0)	2.8 (2.9–2.8)	2.8 (2.9–2.8)	2.4 (2.49–2.40)
Observations	48597	75507	80721	126295
Unique reflections	13513	12363	12762	20215
Completeness	99.2 (95)	92.6 (95)	95.7 (97)	98.1 (99.2)
$I/\sigma(I)$	10.8 (2.5)	8.6 (4.6)	7.3 (3.8)	13.1 (2.1)
R_{sym} (%)	7.0 (53)	10.4 (39)	13.6 (63)	7.2 (70)

Table 3
Equilibrium denaturation parameters for RhoGDI wild type and its mutants.

Mutant	$[GnHCl]_{0.5}$ (*M*)	*m* (kJ mol^{-2})	$\Delta G_{den}^{H_2O}$ (kJ mol^{-1})
Wild type	1.17 ± 0.01	13.1 ± 0.58	15.4 ± 0.75
E87D	0.86 ± 0.01	14.0 ± 0.25	12.1 ± 0.25
E193A	0.87 ± 0.01	14.9 ± 0.25	13.1 ± 0.29
E163A	0.94 ± 0.02	8.96 ± 0.42	8.20 ± 0.54
E87A, E155A	0.94 ± 0.01	13.7 ± 0.46	12.9 ± 0.54
E154A, E155A	0.95 ± 0.01	14.5 ± 0.63	13.8 ± 0.71
E163A, E164A	1.00 ± 0.02	19.0 ± 2.43	19.0 ± 2.72
E87A	1.03 ± 0.01	13.9 ± 0.46	13.4 ± 0.54
E95A	1.07 ± 0.01	13.8 ± 0.46	14.7 ± 0.54
E109A	1.09 ± 0.01	11.4 ± 0.25	12.4 ± 0.29

71 and an *R* factor of 37%. The protein structure was rebuilt using *ARP*/*wARP* (Perrakis *et al.*, 1999) and refined using *REFMAC* (Murshudov *et al.*, 1997) with automated solvent detection. Electron-density maps were visually inspected and minor corrections were applied using *O* (Jones *et al.*, 1991). Individual atomic *B*-factor values were refined isotropically, but the final stage included refinement of anisotropic displacement parameters.

3. Results

3.1. Crystallization screens and diversity of crystal forms

In total, 16 single and multiple mutants were prepared and screened for crystallization (Table 1). Wild-type protein was used as a control and in one isolated case a single crystal grew from solution No. 14 of Crystal Screen II (2.0 *M* ammonium sulfate, 0.1 *M* sodium citrate pH 5.6, 0.2 *M* potassium/sodium tartrate). All mutants but one (E163D) gave hits in both crystallization screens, Crystal Screen I (CSI) and Crystal Screen II (CSII). The most common conditions were those from which wild-type protein grew and No. 26 from CSII, *i.e.* 30% PEG MME 5000, 0.1 *M* MES pH 6.5, 0.2 *M* ammonium sulfate. Two double mutants crystallized from CSI No. 4, which is related to CSII No. 14 in that it contains 2.0 *M* ammonium sulfate. Crystals from these two conditions are isomorphous and belong to space group *R*32 with very close axial lengths (Table 2). However, the kinetics of crystal growth varied significantly between the mutants, with the double mutant E(154,155)A yielding the largest single crystals. It is noteworthy that the morphology of some crystals grown from CSII No. 14 is markedly different, suggesting a different symmetry, although their small size precluded experimental space-group assignment. The crystals grown from CSII No. 26 are all likely to be of the same monoclinic *C*2 form and rather poorly diffracting, although only one mutant (E109A) was evaluated by diffraction. Five mutants gave hits from CSI No. 15 (30% PEG 8000, 0.1 *M* sodium cacodylate pH 6.5, 0.2 *M* ammonium sulfate), which is a set of conditions close to those of CSII No. 26. The morphology of these crystals, all of which were of poor quality and small size, is reminiscent of those from CSII No. 26, suggesting that they too are of the *C*2 type. Thus, all of the mutants (except for E163D) gave crystals of either the *C*2 or the *R*32 form or both.

The triple mutant E(154,155,157)A gave hits in ten different conditions, including seven unique to this mutant. However, they were relatively small and were not used in diffraction studies. In addition, the double mutant E(154,155)A and the single mutant E87A gave crystals from CSI No. 17 (30% PEG 4000, 0.1 *M* Tris–HCl pH 8.5, 0.2 *M* lithium sulfate). The E87A crystals were invariably twinned, but the observed diffraction extended to 2.0 Å or better. We were unable to obtain any single crystals from this mutant and as a result the space group was not determined. The E(154,155)A mutant gave higher quality crystals after some optimization of crystallization conditions and a single crystal was found which exhibited a novel symmetry with a triclinic unit cell and a diffraction pattern extending to very high resolution (beyond 1.2 Å).

3.2. The stability of RhoGDI and various Glu→Xaa mutants

To evaluate the stabilities of selected Glu→Ala and Glu→Asp mutants we monitored chemical denaturation by fluorescence changes. This method leads to a direct determination of the ΔG at room temperature, at which temperature crystallization screens were carried out. Our attempts to use the method of differential scanning calorimetry (DSC), which yields accurate values of the denaturation temperature T_{den}, was made difficult by the fact that thermal denaturation led to some protein aggregation.

Denaturation curves of the GDI wild type and its nine mutants obtained by monitoring the increase in fluorescence are shown in Fig. 2. The solid lines represent the non-linear least-squares best fits of the data to (1). It can be noticed from Fig. 2 and Table 3 that wild-type Δ66 RhoGDI as well as all mutants show relatively low stability compared with other proteins of similar size (Makhatadze & Privalov, 1995). The $\Delta G_{den}^{H_2O}$ value is ~15.4 kJ mol^{-1} [this is consistent with an estimate of T_{den} based on DSC (data not shown) of 321 K]. The destabilization of most of the mutant proteins is manifested by the decrease in $[GnHCl]_{0.5}$ values and changes in

denaturation cooperativity, documented by m values (Table 3). The strongest decrease in stability, by 7.24 kJ mol^{-1}, is observed for the E163A mutant. Interestingly, introduction of another Glu→Ala mutation at an immediately adjacent site provides 10.4 kJ mol^{-1} stabilization energy, resulting in the only mutant which is more stable than the wild type. All other mutants were found to be less stable than the wild type, although in some cases only by a small margin.

3.3. Structure of the E(154,155)A double mutant

The E(154,155)A double mutant crystallized in vapor-diffusion experiments with an optimal reservoir solution of 24% PEG 4000, 100 m*M* Tris pH 8.5, 200 m*M* $LiSO_4$ and 2.5% MPD. Many crystals grown under these conditions diffracted X-rays to high resolution, but were twinned in a visually undetectable manner. However, one comparatively large but imperfectly shaped crystal (0.5 × 0.2 × 0.2 mm) exhibited single-lattice diffraction extending to beyond 1.2 Å. High-quality data were collected and processed to 1.3 Å resolution (Table 4). The crystal belongs to the triclinic *P*1 space group and the unit-cell volume suggested a content of two protein molecules with 49% solvent (V_M = 2.5 Å^3 Da^{-1}). Molecular-replacement calculations readily revealed the positions for two RhoGDI molecules and the model was refined (Table 4). The arrangement of the two molecules in the unit cell is shown in Fig. 3, showing the molecular packing in a layer of the crystalline lattice and highlighting the variation of the atomic *B*-factor values indicative of thermal motion. Superposition of the two molecules (designated *A* and *B*) involves a 180° rotation and a translation and although no restraints were applied for non-crystallographic symmetry during refinement, the root-mean-square difference in the positions for the C^α atoms in the two molecules after alignment is only 0.23 Å, with a maximum difference of 0.67 Å. The interface between the two molecules is well ordered with low *B*-factor values.

Overall, the structure is very similar to previously described crystal structures of the immunoglobulin-like domain of RhoGDI (Longenecker, Garrard *et al.*, 2001; Keep *et al.*, 1997) with structural alignments of C^α atoms, yielding r.m.s. deviations of 0.57 Å compared with the crystal structure of RhoGDI at 2.5 Å resolution (PDB code 1rho, molecule *A*) and 0.54 Å compared with the mutant 2.0 Å structure (PDB code 1fso). Graphing the distances between the C^α atoms for these aligned structures as a function of residue highlights local differences (Fig. 4), the largest of which are notably located at residues involved in intermolecular contacts or in regions subjected to point mutagenesis. For example, a spike above 1 Å deviation is observed for residue 135, a lysine residue that was mutated to alanine in the 1fso structure. Also in comparison with 1fso, a similar deviation is noted for residue 186, which in the triclinic crystal form of the glutamate double mutant participates in a small interface with other molecules related by translational symmetry.

Of particular interest is the packing arrangement of the protein molecules in the triclinic crystal form reported here, revealing the importance of the point mutations for the crystal lattice. The Glu→Ala mutations of residues 154 and 155 allow the side chain of Arg117 to adopt a novel conformation favorable for intermolecular packing (Fig. 5*a*). The guanidinium group of Arg117 interacts closely with the side chains of Ser124 and Ser148 of a neighboring molecule, forming the central portion of the interface between molecules *A* and *B*. Adjacent to this interaction, the N-terminus of molecule *A* lays against molecule *B*, forming a hydrogen bond between the main-chain atoms Val*A*67 NH and CO of Glu*B*157 (3.1 Å), with the side chain of Val67 fitting into a hydrophobic pocket of molecule *B* (Fig. 5*b*). Ordered solvent molecules provide additional bridging interactions across this interface. The packing within the lattice is such that the interactions of molecule *A* with molecule *B* are repeated for molecule *B* interacting with a crystallographically related copy of molecule *A* translated by one unit-cell length.

In our previous report describing the effects of Lys→Ala mutations on the crystallization of RhoGDI (Longenecker, Garrard *et al.*, 2001), we noted the propensity of RhoGDI molecules to form dimers within various crystal lattices. Typically, Leu170 from one molecule fills the entrance to the hydrophobic pocket of a neighboring molecule in a symmetrical arrangement to form a dimer. Minor variations on this general feature result in different angles between the molecules in the various crystal forms. In striking contrast to this arrangement, the molecules of the E(154,155)A mutant pack together, leaving the hydrophobic pocket open to solvent. In fact, the 170-loop does participate in intermolecular contacts, but in this case residues 169–170 form a small interface with residues 99, 100 and 195 of an adjacent molecule. The hydrophobic pocket, which accommodates the geranylgeranyl moiety of Rho family GTPases in functional interactions in the cell, is filled with ordered solvent molecules and presents a novel snapshot of the cavity without ligand. We note that this will perhaps be useful in structural studies designed to probe the specificity and binding characteristics of various compounds in the hydrophobic cavity.

Table 4
Data-collection and refinement statistics for E(154,155)A.

Values in parentheses are values for the highest resolution shell (1.29–1.25 Å).

X-ray data	
Unit-cell parameters (Å, °)	a = 34.10, b = 35.92, c = 67.51, α = 79.2, β = 82.7, γ = 76.4
Resolution d_{min} (Å)	1.25
Observations	147519
Unique reflections	75214
Completeness (%)	89 (55)
$I/\sigma(I)$	18.6 (3.6)
R_{sym}† (%)	2.1 (14.3)
Structure refinement	
R_{cryst} (%)	15.8
R_{free}‡ (%)	19.5
R.m.s.d. bonds (Å)	0.006
R.m.s.d. angles (°)	2.2
Mean B values (Å^2)	
Protein	18.3
Solvent	38.1

† $R_{sym} = \sum |I - \langle I \rangle| / \sum I$, where I is the integrated intensity for a reflection. ‡ R_{free} is the standard crystallographic R factor, R_{cryst}, but calculated on 5% of the data excluded from the refinement.

3.4. Crystallographic analysis of other RhoGDIΔ66 mutants

X-ray diffraction data were also collected to medium resolution (~3 Å) on crystals of a single mutant E109A, a double mutant E(154,155)A and a triple mutant E(154,155,157)A (Table 2). The E109A mutant crystallized in the monoclinic space group *C*2, with a unit-cell volume indicating multiple copies in the asymmetric unit. Molecular-replacement calculations revealed a solution for the positions of four molecules in the asymmetric unit consistent with rotational symmetry exhibited in Patterson self-rotation calculations and translational non-crystallographic symmetry revealed by a peak in a native Patterson map. The four molecules are arranged as two dimers packed side-by-side and the dimers consist of monomers that associate in the typical fashion noted above, whereby Leu170 occupies the entrance to the hydrophobic cavity of the neighboring molecule. Interestingly, for each monomer, residue 109 is located at the interface between the two dimers and so is likely to promote the growth of this crystal form.

Analysis of the double and triple mutants revealed that both of these crystals belong to space group *R*32 and are isomorphous with crystal structures of two single lysine mutants analyzed previously (Longenecker, Garrard *et al.*, 2001) and with the wild-type crystal. Residues 154, 155, and 157 are not located at intermolecular contacts in this *R*32 crystal form and cannot directly impact on the formation of crystal contacts. However, changes in the dipole moment and solubility of the protein may indirectly promote crystal growth in preference to the wild type.

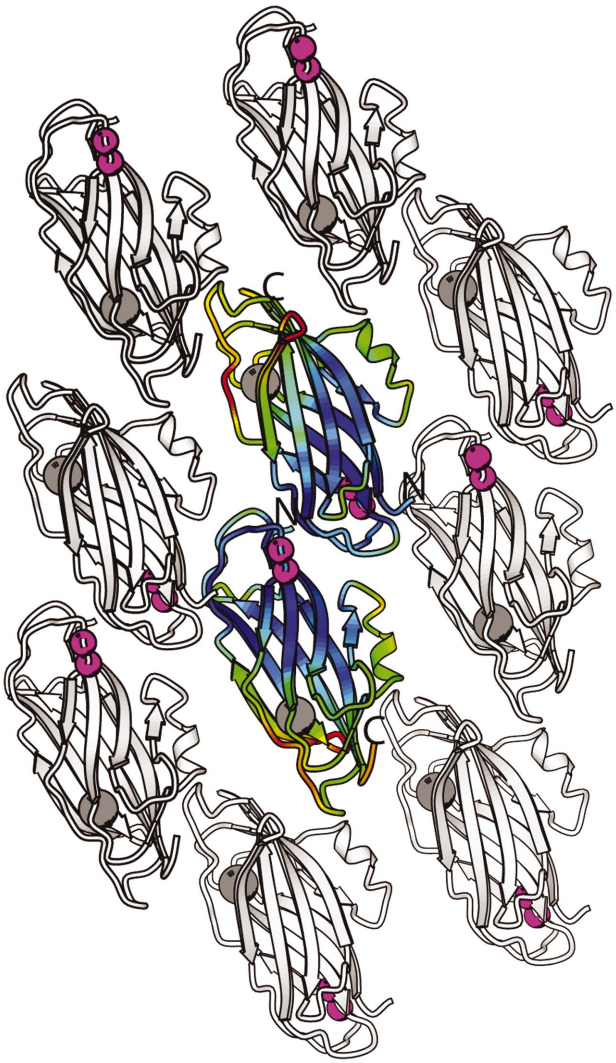

Figure 3
Ribbon diagram of the overall arrangement of the molecules in the asymmetric unit, with the location of the point mutations identified by magenta spheres. The two molecules within the asymmetric unit are colored according to the temperature factors. The grey sphere indicates the entrance to the hydrophobic pocket. The figure was prepared using *BOBSCRIPT* (Esnouf, 1997).

4. Discussion

4.1. Enhanced crystallizability of Glu→Xaa mutants of RhoGDI

In the present study, glutamate residues were chosen as targets for mutagenesis with the objective of testing the hypothesis that their replacement by residues with lower conformational entropy will yield protein with enhanced crystallization potential. Mutations of two types, Glu→Ala and Glu→Asp, were systematically introduced into the RhoGDIΔ66 variant, identical to the protein used to evaluate the impact of Lys→Ala mutations in our previous study (Longenecker, Garrard *et al.*, 2001). Substituting Glu with Ala results in a reduction of total surface conformational entropy, although at the expense of charge removal and possible destabilization. Mutants of the second type, Glu→Asp, were prepared to test the impact of limited entropy reduction without removing a charge. The selection of single mutants which were designed and prepared was not influenced by the structural context, except for Glu163, a relatively rare example of a partly buried glutamate with important structural function: it reaches across the entrance to the hydrophobic pocket between the two β-sheets to form a hydrogen bond with Tyr144. We used Glu163 as an additional negative control, as our assumption is that mutation of partly buried residues should not impact on crystallization.

In earlier studies of Lys→Ala mutants, it was found that multiple mutations are more effective than single ones and lead to the formation of epitopes which are involved in the crystal contacts (Longenecker, Garrard *et al.*, 2001). To test this observation, multiple mutants were prepared in two different ways: one type with mutated residues in close proximity in the primary sequence and a second one with mutated residues distant in the sequence, *e.g.* mutant E(87,155)A, but within a single epitope.

At first glance, the results are most encouraging, because with the exception of the E163D, all mutants gave hits in the two Crystal Screens. A closer examination reveals a more complex picture. Most of the mutants crystallize in one of two forms: a *C*2 cell with four molecules in the asymmetric unit and an *R*32 cell with two molecules. The latter unit cell was also observed for the wild-type Δ66 construct and has been

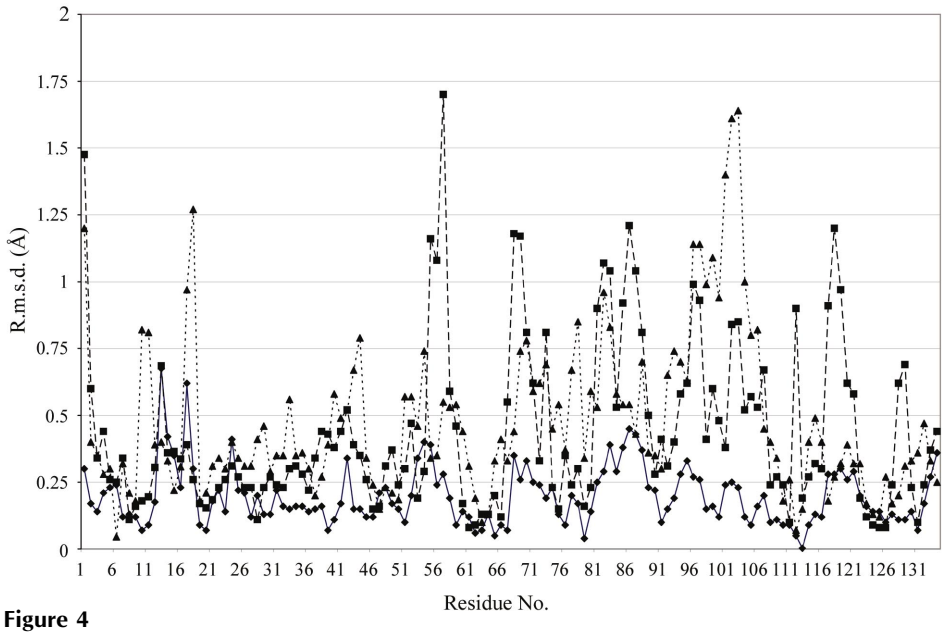

Figure 4
Comparison of the distances between the C^{α} atoms in selected structures of the RhoGDI, superposed by least-squares (all C^{α} atoms), as a function of the amino-acid sequence (consecutive numbering). The solid line and diamonds indicate the difference between the two molecules in the asymmetric unit of the *P*1 high-resolution form; the long dashes and squares show the difference between molecule *A* and the 2.0 Å resolution structure of the quadruple mutant reported previously (Longenecker, Garrard *et al.*, 2001); short dashes and triangles shows the difference between molecule *A* and molecule *A* from the original 2.5 Å resolution structure of Keep *et al.* (1997).

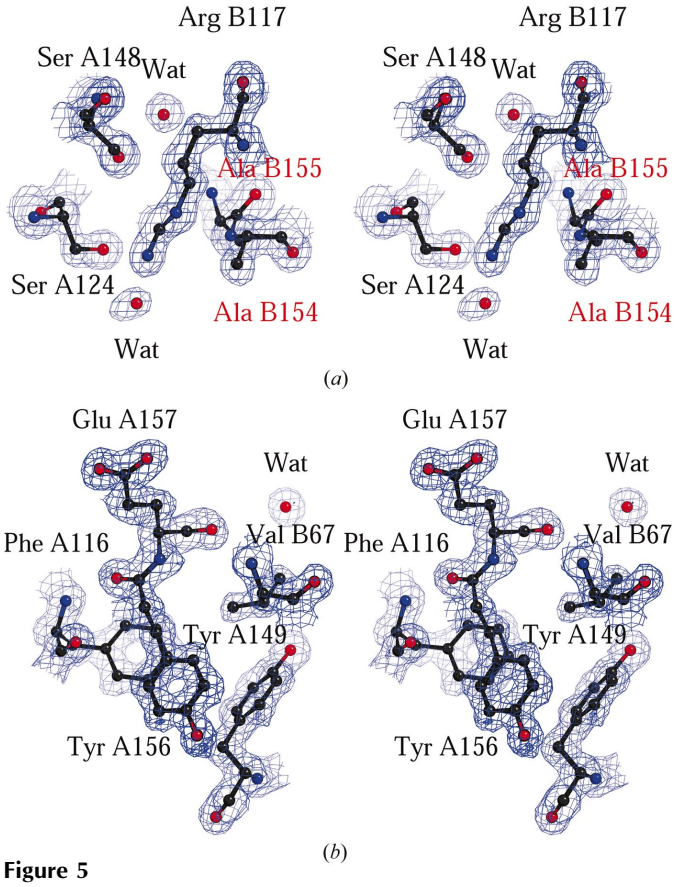

Figure 5
Eectron-density maps. (*a*) At the region of crystal contact involving the mutated sites at 154 and 155. (*b*) At the region of crystal contact involving Tyr149 and Tyr156, and Val67 from the adjacent subunit. The figure was prepared using *BOBSCRIPT* (Esnouf, 1997).

reported by us previously for the K113A and K141A mutants. It has now become clear that RhoGDIΔ66 has a strong propensity to form the *R*32 cell and single mutants only change the growth kinetics, not affecting the type of crystal lattice. Crystals grown from CSI No. 4 show the same symmetry and a total of six mutants yield this type of crystals. The *C*2 form, observed using PEGs as precipitants, is closely related to the *R*32 cell and a slight change in crystallization conditions results in a change from one to the other. We noted that the E87D mutant crystallized readily from CSII No. 26, typical conditions for *C*2, but the crystals were of inadequate quality for diffraction experiments. Optimization experiments using small amounts of additives (*e.g.* 2.5% MPD) produced a dramatic transition to the *R*32 form, without any trace of *C*2 crystals. Of the 16 mutants investigated, 11 yielded *C*2 crystals from the CSI No. 26 conditions or a related solution (CSI No. 15). All tested mutants, with the exception of E163D, which yielded no crystals, produced either *C*2 or *R*32 crystals, albeit with different growth kinetics and different crystal quality and size.

The most dramatic results were observed for the triple mutant E(154,155,157)A, which crystallized from ten different solutions, although in most cases the morphology was reminiscent of either of the two forms described above. Finally, E87 and E(154,155)A gave crystals from a mixture of PEG 4000 and Li_2SO_4 (CSI No. 17); those from the double mutant were shown to exhibit the symmetry of space group *P*1 and were subsequently used to collect the 1.3 Å data, although we cannot exclude the possibility that the E87D mutant crystallizes in the same form.

The data presented in this study combined with earlier experiences of using Lys$\rightarrow$Ala mutants for RhoGDI seem to indicate that while single and even double mutants tend to have a significant impact on the crystallization behavior, they do not necessarily induce crystal forms completely inaccessible to the wild-type protein. However, double and triple mutants are much more likely to produce new crystal forms with completely novel packing arrangements and superior diffracting qualities. We note that double and triple mutants have the potential to form epitopes, which directly mediate crystal contacts, in contrast to single mutants, which affect the crystallization kinetics but do not impact on the nature of the contacts.

When working with a new protein for which no structural information is available, the sites for mutagenesis can be selected based on sequence alone, wherever there is a cluster

of Lys and/or Glu residues in close proximity. If our recent successful crystallization of an RGSL domain by this approach (Longenecker, Lewis *et al.*, 2001; Garrard *et al.*, 2001) were to serve as a representative example, as few as five cluster mutations may have to be screened to produce good-quality crystals in a medium-size protein.

4.2. Enhancement of resolution

Our original aim was to test the hypothesis that surface mutagenesis targeting Lys and Glu residues increases the likelihood of obtaining X-ray quality crystals. However, our results indicate that rational surface mutagenesis may yield an additional advantage: even if the wild-type protein does produce medium-quality crystals, new crystal forms generated in this fashion may have superior qualities and diffract to much higher resolution. The original study of the immunoglobulin domain of RhoGDI was conducted at 2.5 Å resolution. The wild-type crystal of this domain reported here yielded similar quality data to 2.4 Å. However, our recent study identified a triple mutant K(135,138,141)A which crystallized in space group $P3_22_12$ and diffracted to 2.0 Å in spite of a very high solvent content. In this study, we describe a double mutant E(154,155)A (space group $P1$) which diffracts to beyond 1.2 Å and for which very high quality 1.3 Å data were processed. In both cases, the mutations resulted in a protein with marked decrease in stability. This demonstrates that the crystal lattice defined by intermolecular contacts is the primary determinant of the quality of protein crystals. While thermophilic proteins are easier to work with for diverse reasons, they probably should not be chosen for crystallographic studies exclusively because of their perceived potential to crystallize better than less stable orthologues.

4.3. Stability of RhoGDIΔ66 and its surface mutants

Our study also included the first rigorous assessment of the stability of the RhoGDI molecule and of its mutants. One of the potential side effects of surface mutagenesis is destabilization of the protein fold or the reduction of the free-energy difference ΔG between the folded and unfolded states. Given the apparent consensus that more thermostable proteins are better suited for crystallographic analysis, we were concerned that destabilization caused by surface mutations may adversely affect the quality of crystals and success rate of crystallization. Our study revealed that the immunoglobulin domain of RhoGDI is significantly less stable at room temperature than other proteins of similar size, with a $\Delta G_{\rm den}^{\rm H_2O}$ value of $\sim$15.4 kJ mol^{-1}. The unfolded N-terminal fragment has little impact on the stability, as the $T_{\rm den}$ of the Δ23 variant, as estimated by DSC (data not shown) is nearly identical to that of the Δ66 variant.

While nearly all mutations studied destabilize the RhoGDI molecule, the most adverse effect is observed for the E163A mutation. This is very interesting because Glu163 is the only partly buried glutamate in the structure, extending across the entrance to the far end of the prenyl-binding pocket and forming a strong hydrogen bond with Tyr144 from the opposing β-sheet (Glu163 O$^{\varepsilon 2}\cdots$Tyr144 O$^{\eta}$). We originally chose the E163A mutant as an additional control because a mutation at this position was not expected to result in any significant change in the crystallization properties. Clearly, breaking the hydrogen bond linking the two β-sheets is deleterious to the stability of the fold. Interestingly, introduction of yet another Glu→Ala mutation at an immediately adjacent site (164) provides 10.8 kJ mol^{-1} stabilization energy to the double mutant E163A,E164A, resulting in the only mutant that is more stable than the wild type (Table 3). The increase in stability observed for the E163A,E164A double mutant may be related to the elimination of the electrostatic repulsion between neighboring side chains of Glu164 and Glu109, located on the outer surface of the β-sheet.

4.4. The high-resolution structure of RhoGDIΔ66 (E154,155A) double mutant

RhoGDI, the guanine nucleotide dissociation inhibitor of Rho GTPases, is a physiologically important down-regulator of RhoA, Rac, Cdc42 and related proteins. It has been a subject of numerous studies, both in its apo-type form as well as in complexes with GTPases. RhoGDI is made up of three distinct regions: a 23-residue long N-terminal sequence with no apparent biological or structural properties; an $\sim$40-residue-long polypeptide unstructured in solution and folded into two helices in complexes with target GTPases; and an immunoglobulin-like domain which binds to Rho *via* a surface epitope and which sequesters the prenyl moiety in a cavity formed between the two β-sheets. The apo-structure of the immunoglobulin domain was characterized by NMR and X-ray diffraction, although the relatively poor quality of the crystals limited the resolution to 2.5 Å, thus precluding the possibility of a detailed assessment of some of the features, such as solvation within the cavity, exact stereochemistry of hydrogen bonding *etc*. Our present study resulted in the preparation of high-quality crystals of RhoGDIΔ66 and allowed us to refine the structure at 1.3 Å resolution using anisotropic displacement parameters. The refined model yields more accurate insight into some aspects of the structure–function relationships.

It was noted previously that upon prenyl binding RhoGDI undergoes expansion as the two β-sheets separate to accommodate the bound lipid (Grizot *et al.*, 2001; Hoffman *et al.*, 2000). This was based on a comparison of complexed species with the only available uncomplexed structure (Keep *et al.*, 1997), which might have been potentially influenced by crystal contacts or crystallization conditions. Our present study, as well as previous results with Lys→Ala mutants (Longenecker, Garrard *et al.*, 2001), indicate that RhoGDI has a structurally robust fold which is not affected in any significant way by crystal contacts and that the separation of the β-sheets in the apo-protein is constant.

The high-resolution crystal structure of the E(154,155)A double mutant allows for the first time a reliable analysis of the solvent structure at the entrance to and within the hydrophobic cavity of RhoGDI. This is possible because the

entrance is not obstructed in the P1 form by crystal contacts, as is the case with virtually all other crystal forms of the apo protein studied to date.

5. Conclusions

The results presented in this paper provide further support for the proposal that rational surface mutagenesis should be regarded as a useful tool in the preparation of suitable X-ray quality protein crystals. The Glu→Ala mutations appear to have enhanced the probability of RhoGDI forming crystals, although the effects were not as dramatic as those reported by us previously for the Lys→Ala mutants. The Glu→Asp mutations seem to have much less of an impact, although the smaller number of mutants investigated precludes more general conclusions. Several observations are worth special emphasis. Single mutants often dramatically change the kinetics of crystal nucleation and/or growth, even though the crystal form may be the same as for the wild type. Therefore, these mutations may be useful when wild-type crystals are poorly reproducible or small. Multiple mutations occurring in clusters are very likely to generate novel crystal forms and may be routinely used for proteins recalcitrant to crystallization or in cases where the quality of wild-type crystals is inadequate. It is highly probable that the cluster mutations may mediate novel crystal contacts. We note that this conclusion is supported not only by our studies of the RhoGDI mutants, but also by the application of the strategy to the RGSL domain of PDZRhoGEF (Longenecker, Lewis *et al.*, 2001; Garrard *et al.*, 2001). Finally, the high-resolution structure of RhoGDI reported in this paper illustrates that crystal contacts appear to be the principal determinant of the quality of the crystals as measured by the resolution. This is a particularly important observation, because it has often been thought that the nature of the protein, particularly its stability, has a critical impact on the quality of the crystals and therefore the resolution of the diffraction data. This is one of the reasons why proteins from thermophiles are often preferred targets for crystallographers. Our work demonstrates that even destabilizing mutations can generate crystal-forming epitopes, which lead to crystals of superior quality compared with wild-type proteins. This phenomenon has also been recognized recently with respect to membrane proteins (Camara-Artigas *et al.*, 2001).

We note that of the nearly 13 500 crystallographic entries in the Protein Data Bank, over 2500 (18.5%) are based on data collected to a resolution of 2.5 Å or worse. Many of these entries refer to proteins or complexes of unique biological significance. Given the comparative ease (by use of modern molecular-biology techniques) of making specific surface mutations such as those suggested here and the potential for dramatic improvements in resolution as a result, it may be worthwhile to continue attempts to improve crystal quality by use of these methods rather than settle for the medium- or low-resolution data obtained from the first crystals grown.

This study was funded in part by the NIGMS (Grant GM62615 to ZSD). Jacek Otlewski is a Scholar of the Foundation for Polish Science and Daniel Krowarsch is a recipient of the Young Scholar Award from the Foundation for Polish Science.

References

Camara-Artigas, A., Magee, C. L., Williams, J. C. & Allen, J. P. (2001). *Acta Cryst.* D**57**, 1281–1286.
Carson, M. (1991). *J. Appl. Cryst.* **24**, 958–961.
Esnouf, R. M. (1997). *J. Mol. Graph.* **15**, 132–143.
French, G. S. & Wilson, K. S. (1978). *Acta Cryst.* A**34**, 517–525.
Garrard, S. M., Longenecker, K. L., Lewis, M. E., Sheffield, P. J. & Derewenda, Z. S. (2001). *Protein Expr. Purif.* **21**, 412–416.
Grizot, S., Faure, J., Fieschi, F., Vignais, P. V., Dagher, M. C. & Pebay-Peyroula, E. (2001). *Biochemistry*, **40**, 10007–10013.
Hoffman, G. R., Nassar, N. & Cerione, R. A. (2000). *Cell*, **100**, 345–356.
Jones, T. A., Zou, J. Y., Cowan, S. W. & Kjeldgaard, M. (1991). *Acta Cryst.* A**47**, 110–119.
Keep, N. H., Barnes, M., Barsukov, I., Badii, R., Lian, L. Y., Segal, A. W., Moody, P. C. E. & Roberts, G. C. K. (1997). *Structure*, **5**, 623–633.
Kendrew, J. C., Parrish, R. G., Marrack, J. R. & Orlans, E. S. (1954). *Nature (London)*, **174**, 946–949.
Longenecker, K. L., Garrard, S. M., Sheffield, P. J. & Derewenda, Z. S. (2001). *Acta Cryst.* D**57**, 679–688.
Longenecker, K. L., Lewis, M. E., Chikumi, H., Gutkind, J. S. & Derewenda, Z. S. (2001). *Structure*, **9**, 559–569.
Makhatadze, G. I. & Privalov, P. L. (1995). *Adv. Protein Chem.* **47**, 307–425.
Murshudov, G. N., Vagin, A. A. & Dodson, E. J. (1997). *Acta Cryst.* D**53**, 240–255.
Navaza, J. (1994). *Acta Cryst.* A**50**, 157–163.
McElroy, H. H., Sisson, G. W., Schottlin, W. E., Aust, R. M. & Villafranca, J. E. (1992). *J. Cryst. Growth*, **122**, 265–272.
Otterbein, L. R., Graceffa, P. & Dominguez, R. (2001). *Science*, **293**, 708–711.
Otwinowski, Z. & Minor, W. (1997). *Methods Enzymol.* **276**, 307–326.
Perrakis, A., Morris, R. & Lamzin, V. S. (1999). *Nature Struct. Biol.* **6**, 458–463.
Rayment, I., Rypniewski, W. R., Schmidt-Base, K., Smith, R., Tomchick, D. R., Benning, M. M., Winkelmann, D. A., Wesenberg, G. & Holden, H. M. (1993). *Science*, **261**, 50–58.
Santoro, M. M. & Bolen, D. W. (1992). *Biochemistry*, **31**, 4901–4907.
Sheffield, P. J., Garrard, S. M. & Derewenda, Z. S. (1999). *Protein Expr. Purif.* **15**, 34–39.